Electronic Supplementary Material (ESI) for Journal of Materials Chemistry A.

Supporting information for

Engineering Hierarchical Sb_2S_3/N-C from Nature Minerals with Stable Phase-change towards All-climate Energy Storage

Figures and Captions

Fig. S1 The SEM images of SS-OM (a, d), SS-SO (b, e) and SS-NC (c, f)

Fig. S2 The TEM of SS-OM(a), SS-SO(b) and SS-NC (c)

Fig. S3 Contact angle measurement: for SS-OM (a), SS-NC (b)

Fig. S4 The electrochemical properties of three samples at 0.5 A g^{-1} during 150 cycles: cycling stability (a), capacity retention (b).

Fig. S5 The electrochemical properties of full cell about LiFePO4 vs. SS-NC: cycling stability (a), rate abilities(b), charge-discharge platforms at different cycles (c), differential median curves (d).

Fig. S6 The multi-cycling CV curves from 1st to 5th at 0.3 mV s^{-1} of SS-OM (a) and SS-SO (b)

Fig. S7 Various CV curves at 2.0 mV s^{-1} of SS-OM (a) and SS-SO (b)

Fig. S8 the log(v) versus log(i) for peak1 of the as-targeted samples (a), the ratio of capacitive contributions at 0.3 mV s^{-1} for SS-OM (b) and SS-SO (c)

Fig. S9 the Nyquist plots of SS-OM (a) and SS-SO (b)

Fig. S10 the Nyquist Plots and relative fitting circuit at 50^{th} of these three as-samples

Fig. S11 the linear relations of Z'' vs. $\omega^{-1/2}$ for SS-OM (a) and SS-SO (b), the relationships of Phase Angle vs. Frequency of SS-OM (c) and SS-SO (d).

Fig. S12 the D_{Li+} values during the charge process for these three as-samples

Fig. S13 The electrochemical properties at low temperatures: their cycling properties at 0.5 A g^{-1} (a) and 1.0 A g^{-1} (d), the comparison of charge/discharge platforms at RT/LT for SS-OM (b) and SS-SO (c), their linear relationship of I_p versus $v^{1/2}$ at Peak1/3 (e),

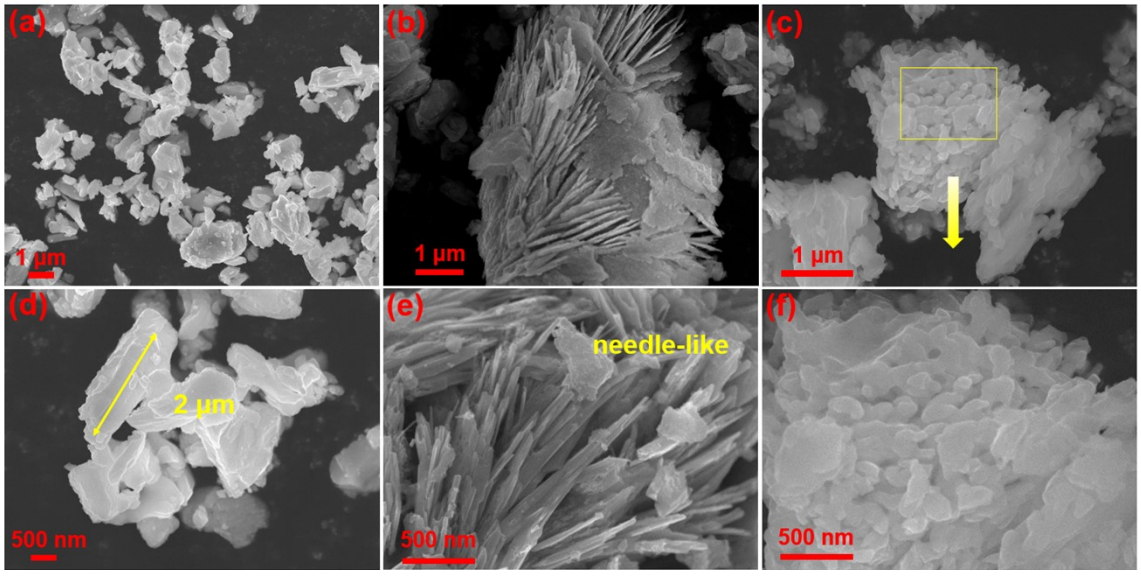

Fig. S1 The SEM images of SS-OM (a, d), SS-SO (b, e) and SS-NC (c, f)

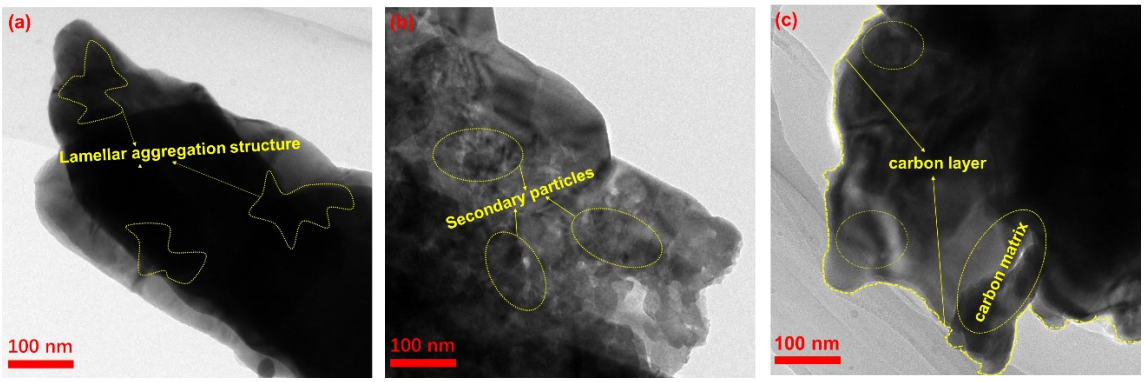

Fig. S2 The TEM of SS-OM(a), SS-SO(b) and SS-NC (c)

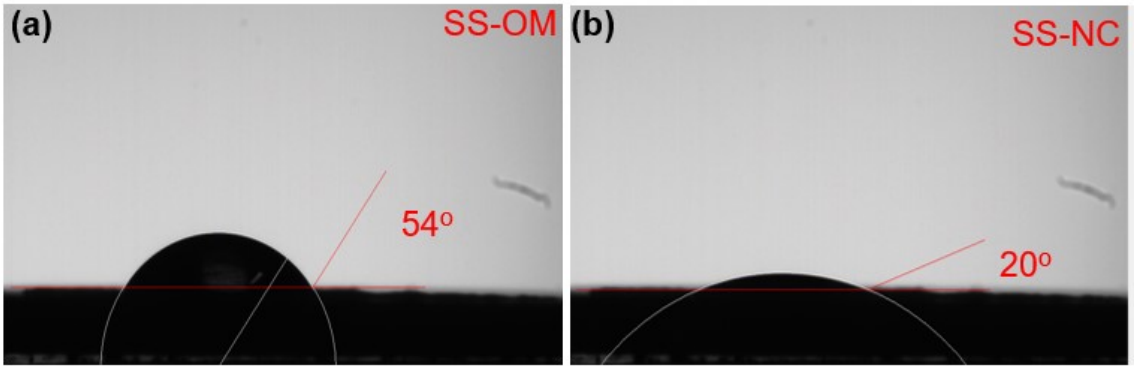

Fig. S3 Contact angle measurement: for SS-OM (a), SS-NC (b)

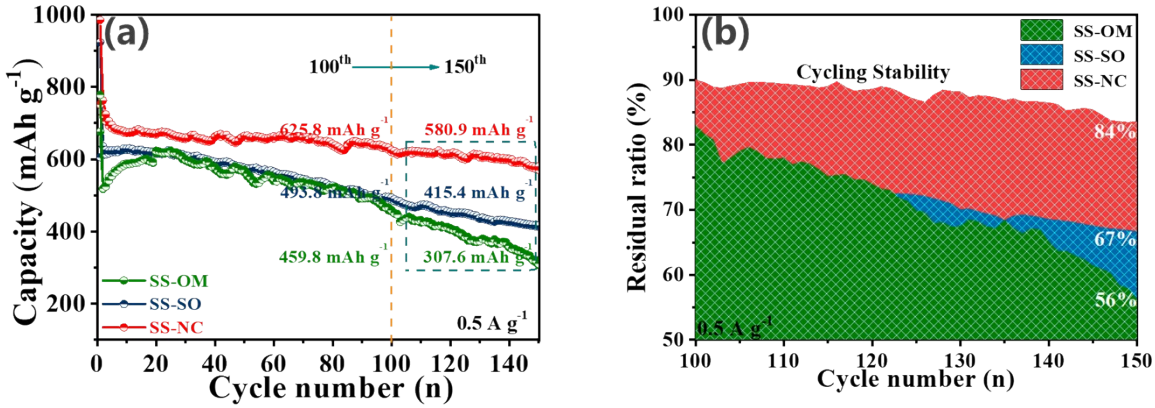

Fig. S4 The electrochemical properties of three samples at 0.5 A g-1 during 150 cycles : cycling stability (a), capacity retention (b).

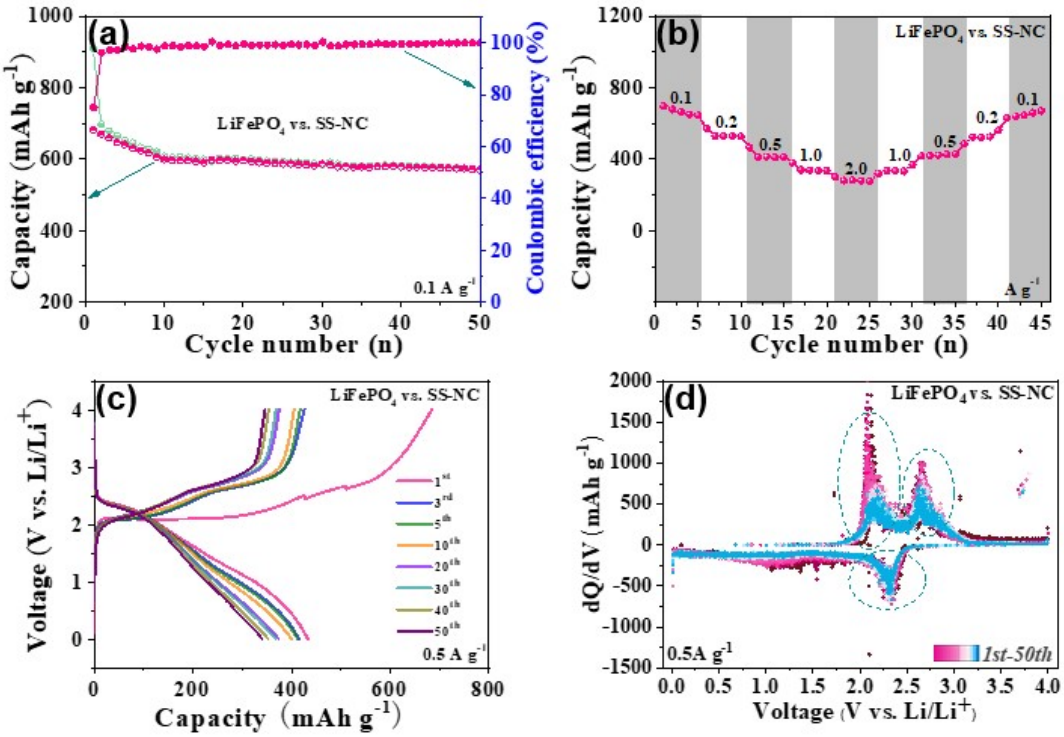

Fig. S5 The electrochemical properties of full cell about $LiFePO_4$ *vs.* SS-NC: cycling stability (a), rate abilities(b), charge-discharge platforms at different cycles (c), differential median curves (d).

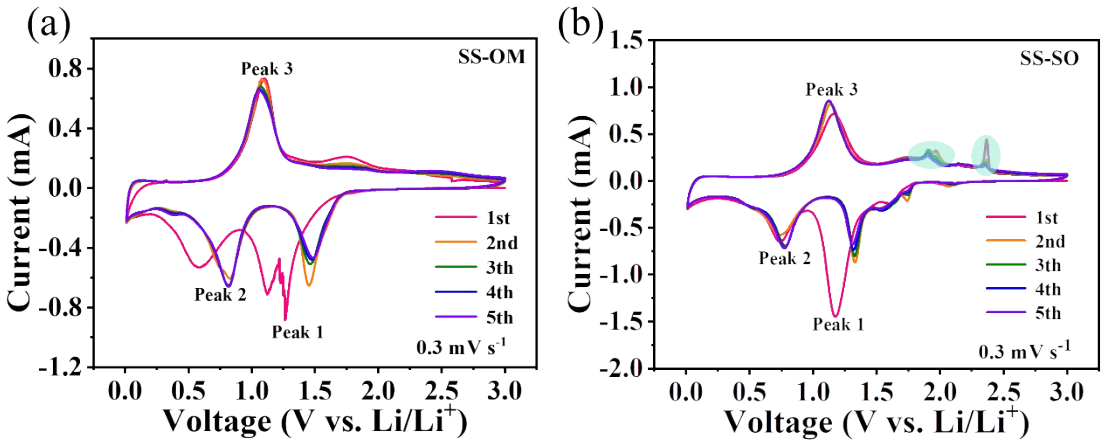

Fig. S6 The multi-cycling CV curves from 1st to 5th at 0.3 mV s^{-1} of SS-OM (a) and SS-SO (b)

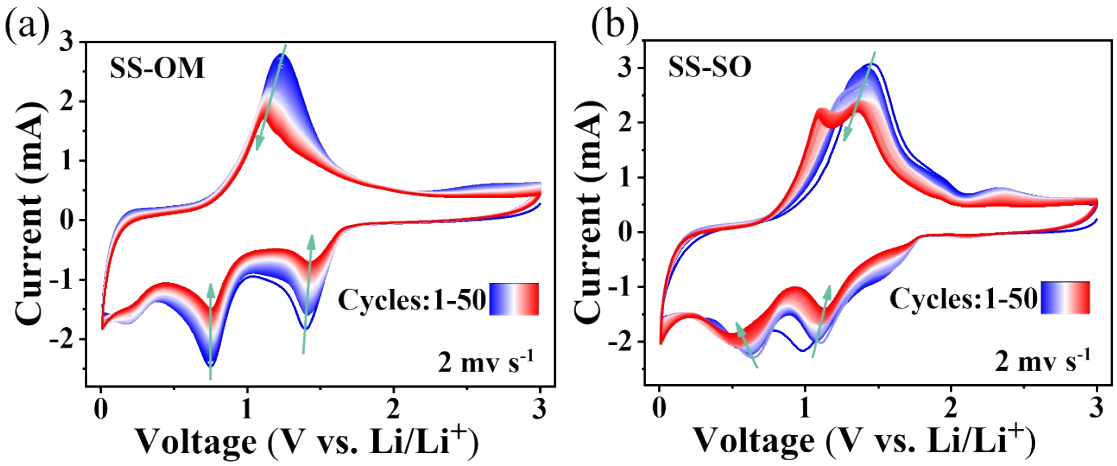

Fig. S7 Various CV curves at 2.0 mV s^{-1} of SS-OM (a) and SS-SO (b)

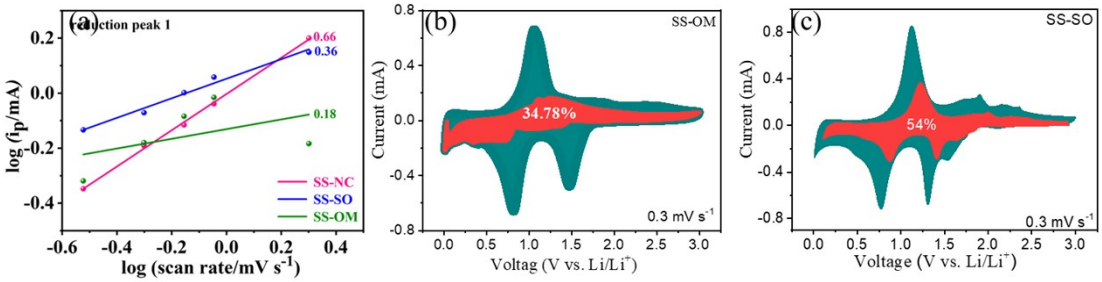

Fig. S8 the log(v) versus log(i) for peak1 of the as-targeted samples (a), the ratio of capacitive contributions at 0.3 mV s^{-1} for SS-OM (b) and SS-SO (c)

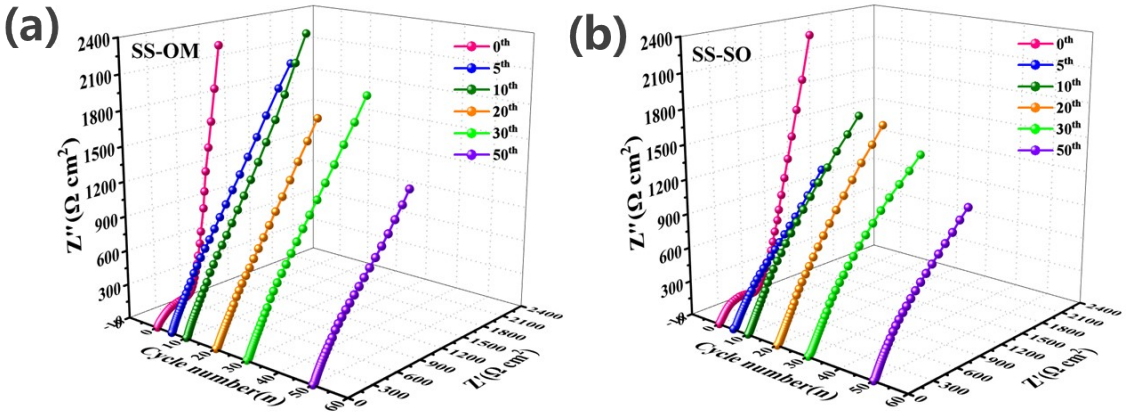

Fig. S9 the Nyquist plots of SS-OM (a) and SS-SO (b)

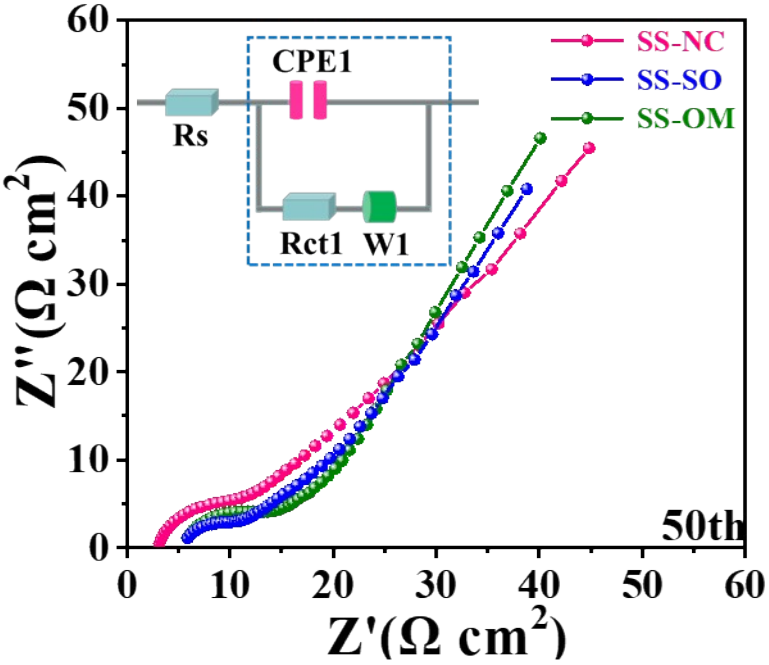

Fig. S10 the Nyquist Plots and relative fitting circuit at 50th of these three as-samples

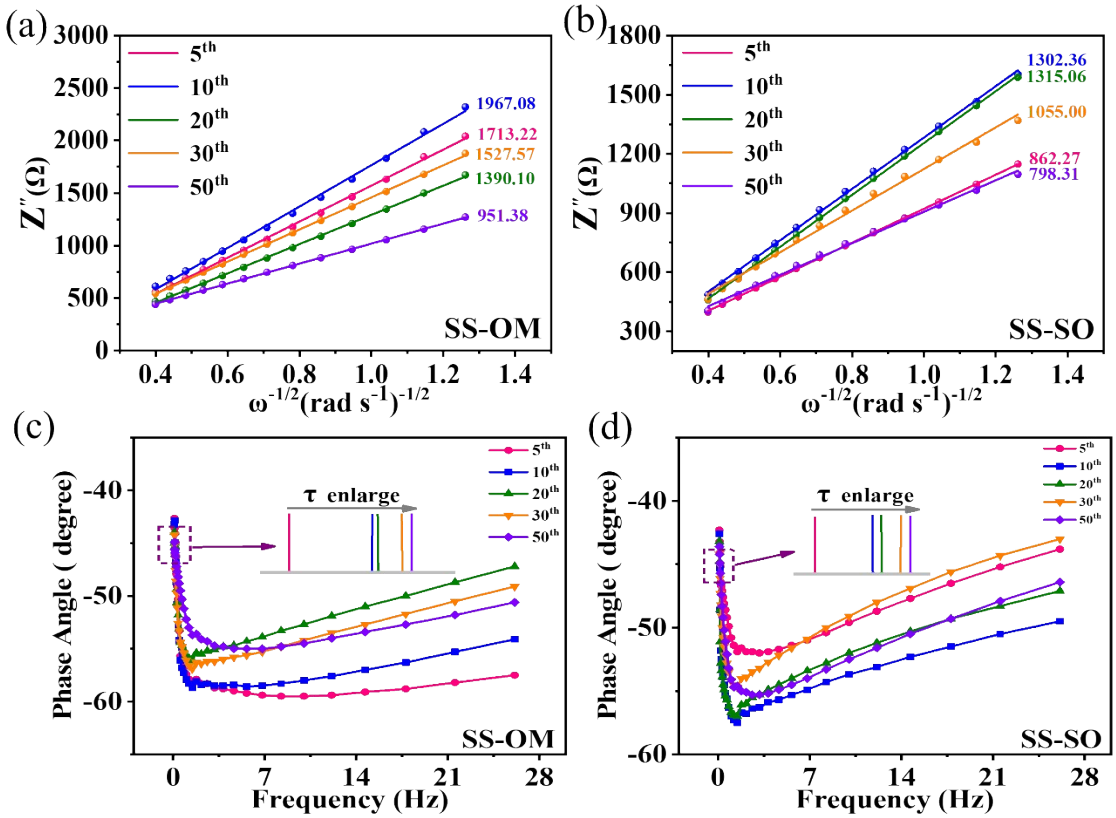

Fig. S11 the linear relations of Z'' vs. $\omega^{-1/2}$ for SS-OM (a) and SS-SO (b), the relationships of Phase Angle vs. Frequency of SS-OM (c) and SS-SO (d).

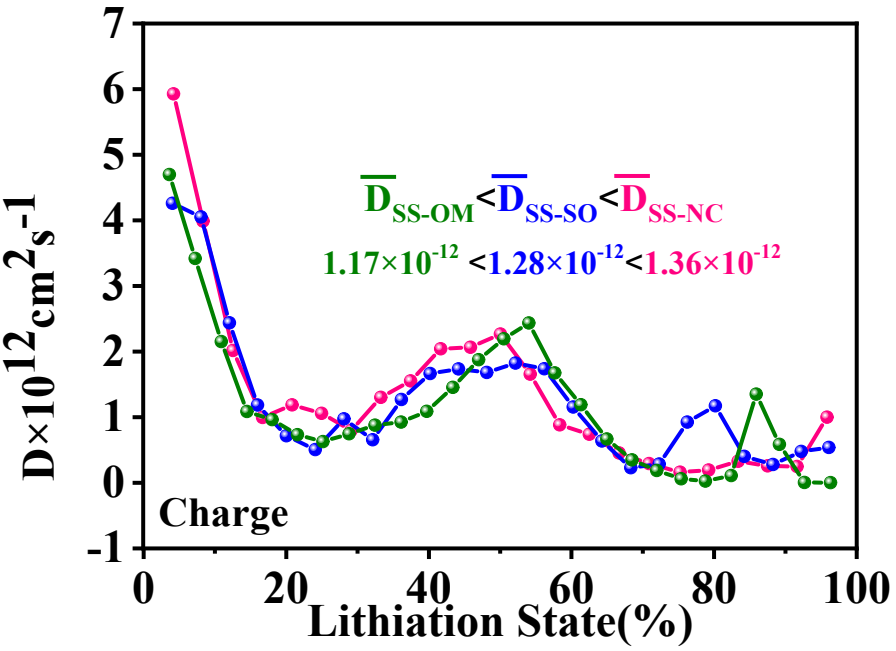

Fig. S12 the D_{Li+} values during the charge process for these three as-samples

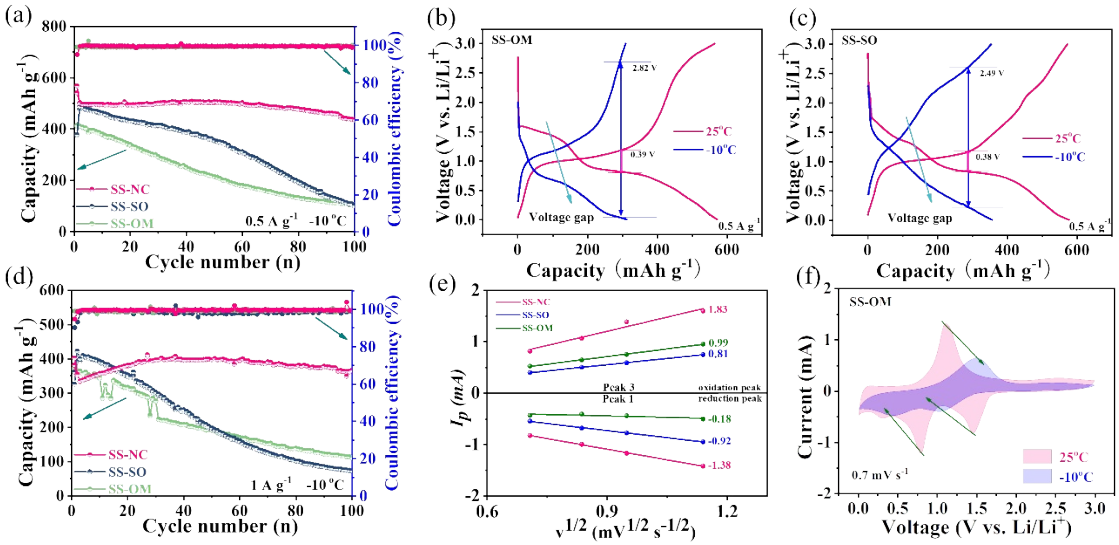

Fig. S13 The electrochemical properties at low temperatures: their cycling properties at 0.5 A g^{-1} (a) and 1.0 A g^{-1} (d), the comparison of charge/discharge platforms at RT/LT for SS-OM (b) and SS-SO (c), their linear relationship of I_p versus $v^{1/2}$ at Peak1/3 (e), the analysis of CV curves at RT/LT (0.7 mV s^{-1}) for SS-OM (f).

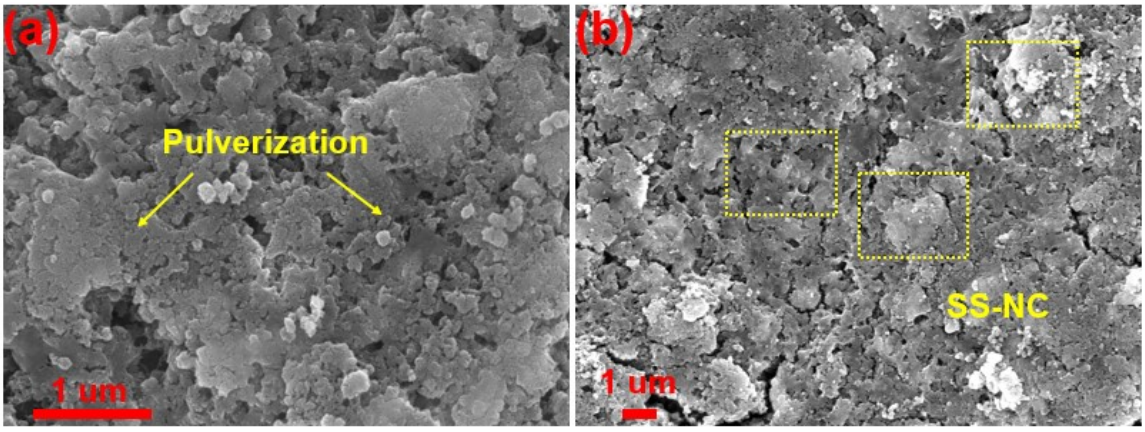

Fig. S14 SEM images avout the electrodes after 100 cycles: SS-OM (a), SS-NC (b).

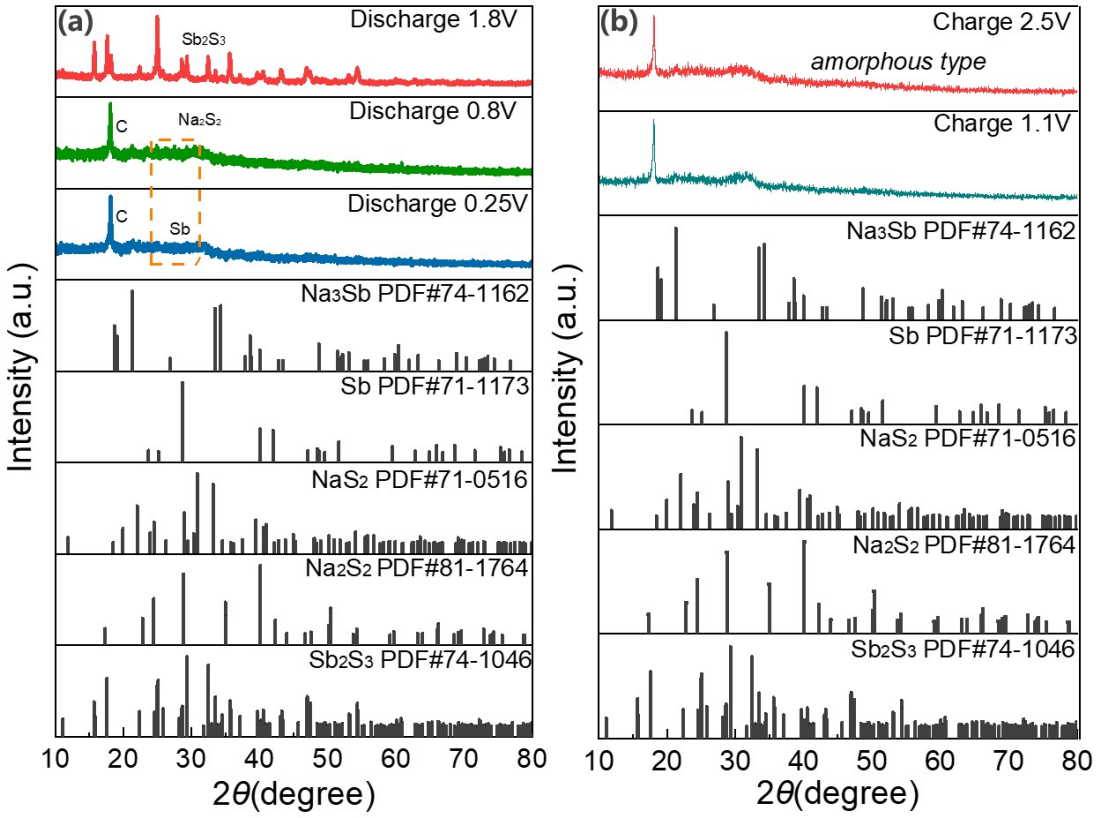

Fig.S 15 Ex-situ XRD patterns of SS-NC

Table S1 The content for all elements in the SS-NC material

Atoms	*S2p*	*C1s*	*N1s*	*Sb3d*	*O1s*
Atomic content (%)	*38.9*	*22.05*	*8.99*	*24.71*	*1.96*

Table S2 The electrochemical properties of Sb_2S_3 samples from the previous reports.

Materials	***Voltage (V)***	***Temperature (°C)***	***Capacity (cycle number) at A g^{-1}***	***capacity retention (%)***	***Ref.***
Sb_2S_3 /lotus-polle	0.01-2.50	~	591 (100) at 0.1	59.8	Ref [1]
Sb_2S_3/MHCS nanospheres	0.01-3.00	~	745.3 (160) at 0.1	59.6	Ref [2]
Sb_2S_3/MMCN	0.01-3.00	room temperature	226.0 (100) at 0.1	39.0	Ref [3]
Sb_2S_3/ppy	0.01-3.00	room temperature	389.0 (160) at 0.1	83.0	Ref [3]
Sb_2S_3/MMCN @ppy	0.01-3.00	room temperature	827.0 (100) at 0.1	92.0	Ref [3]
Sb_2S_3/CS	0.01-2.50	25	566 (200) at 0.2	63.2	Ref [4]
Few-layer 2D Sb_2S_3(2D-SS)	0.01-3.00	~	607 (200) at 0.2	60.9	Ref [5]
p-Sb_2S_3(ss)	0.01-3.00	room temperature	311 (50) at 0.1	41.5	Ref [6]
rGO/Sb_2S_3(ss)	0.01-3.00	room temperature	596 (50) at 0.1	62.7	Ref [6]
rGO/Sb_2S_3(ht)	0.005-3.00	room temperature	658 (50) at 0.1	48.7	Ref [6]
bundle-like Sb_2S_3	0.01-3.00	~	548 (100) at 0.1	79.8	Ref [7]
Sb_2S_3/G	0.01-3.00	room temperature	670 (200) at 0.2	89.3	Ref [8]
rGO-Sb2S3-0.5h	0.00-2.50	~	750 (50) at 0.25	82.5	Ref [9]

rGO-Sb2S3-5.0h	0.00-2.50	~	750 (50) at 0.25	90.0	Ref [9]
Sb_2S_3-Co_9S_8/NC	0.01-3.00	~	715 (100) at 0.2	71.5	Ref [10]
CNN@Sb_2S_3	0.01-3.00	ambient temperature	953 (100) at 0.2	~	Ref [11]
Sb_2S_3/CNT	0.01-3.00	~	443 (100) at 0.2	47.6	Ref [12]
20-25 nm colloidal Sb_2S_3 nanoparticles (NPs)	0.10-2.00	~	408.1 (1200) at 2.4	55.0	Ref [13]
Sb_2S_3 nanorods	0.00-2.50	room temperature	298.6 (20) at 0.3375	28.6	Ref [14]
This work	0.01-3.0	-10	366.9 (100) at 1.0	90.1	

Reference:

[1] Q. Ru, X. Chen, B. Wang, Q. Guo, Z. Wang, X. Hou, S. Hu, Biological carbon skeleton of lotus-pollen surrounded by rod-like Sb 2 S 3 as anode material in lithium ion battery, Materials Letters, 198 (2017) 57-60.

[2] W. Luo, X. Ao, Z. Li, L. Lv, J. Li, G. Hong, Q.-H. Wu, C. Wang, Imbedding ultrafine Sb2S3 nanoparticles in mesoporous carbon sphere for high-performance lithium-ion battery, Electrochimica Acta, 290 (2018) 185-192.

[3] W. Yin, W. Chai, K. Wang, W. Ye, Y. Rui, B. Tang, A highly Meso@Microporous carbon-supported Antimony sulfide nanoparticles coated by conductive polymer for high-performance lithium and sodium ion batteries, Electrochimica Acta, 321 (2019).

[4] J. Xie, J. Xia, Y. Yuan, L. Liu, Y. Zhang, S. Nie, H. Yan, X. Wang, Sb2S3 embedded in carbon–silicon oxide nanofibers as high-performance anode materials for lithium-ion and sodium-ion batteries, Journal of Power Sources, 435 (2019).

[5] S. Yao, J. Cui, Y. Deng, W.G. Chong, J. Wu, M. Ihsan-Ul-Haq, Y.-W. Mai, J.-K. Kim, Ultrathin Sb2S3 nanosheet anodes for exceptional pseudocapacitive contribution to multi-battery charge storage, Energy Storage Materials, 20 (2019) 36-45.

[6] A.S. Hameed, M.V. Reddy, J.L.T. Chen, B.V.R. Chowdari, J.J. Vittal, RGO/Stibnite Nanocomposite as a Dual Anode for Lithium and Sodium Ion Batteries, Acs Sustainable Chemistry & Engineering, 4 (2016) 2479-2486.

[7] Z. Yi, Q. Han, Y. Cheng, Y. Wu, L. Wang, Facile synthesis of symmetric bundle-like Sb2S3 micron-structures and their application in lithium-ion battery anodes, Chem Commun (Camb), 52 (2016) 7691-7694.

[8] Y. Dong, S. Yang, Z. Zhang, J.M. Lee, J.A. Zapien, Enhanced electrochemical performance of lithium ion batteries using Sb2S3 nanorods wrapped in graphene nanosheets as anode materials, Nanoscale, 10 (2018) 3159-3165.

[9] P.V. Prikhodchenko, J. Gun, S. Sladkevich, A.A. Mikhaylov, O. Lev, Y.Y. Tay, S.K. Batabyal, D.Y.W. Yu, Conversion of Hydroperoxoantimonate Coated Graphenes to Sb2S3@Graphene for a Superior Lithium Battery Anode, Chemistry of Materials, 24 (2012) 4750-4757.

[10] G. Ke, X. Wu, H. Chen, W. Li, S. Fan, H. Mi, Y. Li, Q. Zhang, C. He, X. Ren, Unveiling the reaction mechanism of an Sb2S3-Co9S8/NC anode for high-performance lithium-ion batteries, Nanoscale, 13

(2021) 20041-20051.

[11] Z.Y. Yang, Y.F. Yuan, M. Zhu, S.M. Yin, J.P. Cheng, S.Y. Guo, Superior rate-capability and long-lifespan carbon nanotube-in-nanotube@Sb2S3 anode for lithium-ion storage, Journal of Materials Chemistry A, 9 (2021) 22334-22346.

[12] I. Elizabeth, B.P. Singh, S. Gopukumar, Electrochemical performance of Sb2S3/CNT free-standing flexible anode for Li-ion batteries, Journal of Materials Science, 54 (2019) 7110-7118.

[13] K.V. Kravchyk, M.V. Kovalenko, M.I. Bodnarchuk, Colloidal Antimony Sulfide Nanoparticles as a High-Performance Anode Material for Li-ion and Na-ion Batteries, Sci Rep, 10 (2020) 2554.

[14] K. Xiao, Q.Z. Xu, K.H. Ye, Z.Q. Liu, L.M. Fu, N. Li, Y.B. Chen, Y.Z. Su, Facile Hydrothermal Synthesis of Sb2S3 Nanorods and Their Magnetic and Electrochemical Properties, ECS Solid State Letters, 2 (2013) P51-P54.